Coupling of dynamical micromagnetism and a stationary spin drift-diffusion equation: A step towards a fully self-consistent spintronics framework

Michele Ruggeri[c,*], Claas Abert[a], Gino Hrkac[b,c], Dieter Suess[a], Dirk Praetorius[c]

[a] *Christian Doppler Laboratory of Advanced Magnetic Sensing and Materials, Institute of Solid State Physics, TU Wien, Vienna, Austria.*
[b] *College of Engineering, Mathematics and Physical Sciences, University of Exeter, UK.*
[c] *Institute for Analysis and Scientific Computing, TU Wien, Vienna, Austria.*

Abstract

We consider the coupling of the Landau-Lifshitz-Gilbert equation with a quasilinear diffusion equation to describe the interplay of magnetization and spin accumulation in magnetic-nonmagnetic multilayer structures. For this problem, we propose and analyze a convergent finite element integrator, where, in contrast to prior work, we consider the stationary limit for the spin diffusion. Numerical experiments underline that the new approach is more effective, since it leads to the same experimental results as for the model with time-dependent spin diffusion, but allows for larger time-steps of the numerical integrator.

Keywords: Micromagnetism, Landau-Lifshitz-Gilbert equation, Spintronics, Finite element method.

1. Introduction and mathematical model

The classical theory of micromagnetism models the behavior of ferromagnetic materials for constant temperature far below the Curie point and in the absence of electric currents. To take the interactions between magnetization and spin-polarized currents into account, several extensions of the model based on the concept of spin-transfer have been proposed [1–7]. In this work, we consider the Landau-Lifshitz-Gilbert equation (LLG)

$$\partial_t \mathbf{m} = -\gamma_0 \mathbf{m} \times (\mathbf{H}_{\text{eff}}(\mathbf{m}, \mathbf{f}) + c\mathbf{s}) + \alpha \mathbf{m} \times \partial_t \mathbf{m} \quad \text{in } \Omega_T, \tag{1a}$$

$$\partial_{\mathbf{n}} \mathbf{m} = \mathbf{0} \text{ on } (0,T) \times \partial\Omega, \quad \mathbf{m}(0) = \mathbf{m}^0 \text{ in } \Omega, \tag{1b}$$

where the sought vector field is the normalized magnetization $\mathbf{m} : \Omega_T \to \mathbb{R}^3$ with $|\mathbf{m}| = 1$. In (1a), $\Omega \subset \mathbb{R}^3$ is the volume occupied by some ferromagnetic body, $T > 0$ is some finite time, and $\Omega_T = (0,T) \times \Omega$ is the time-space domain. Moreover, $\gamma_0 > 0$ is the gyromagnetic ratio, $\alpha > 0$ is the Gilbert constant, and the effective field is given by

$$\mathbf{H}_{\text{eff}}(\mathbf{m}, \mathbf{f}) = C_{\text{exch}} \Delta \mathbf{m} + \boldsymbol{\pi}(\mathbf{m}) + \mathbf{f}. \tag{1c}$$

In (1c), the first term is the exchange contribution, with $C_{\text{exch}} = 2A/(\mu_0 M_s) > 0$, $\boldsymbol{\pi}(\mathbf{m})$ collects the $\mathbf{m}$-dependent lower-order contributions (e.g., anisotropy field and stray field), and $\mathbf{f}$ comprises the $\mathbf{m}$-independent contributions (e.g., applied external field). In (1a), $\mathbf{s} : \Omega'_T \to \mathbb{R}^3$ denotes the spin accumulation, $\Omega' \subset \mathbb{R}^3$ is the volume of a conducting body such that $\Omega \subset \Omega'$, $\Omega'_T = (0,T) \times \Omega'$, and $c > 0$ is the corresponding coupling constant. The LLG equation is equipped with homogeneous Neumann boundary conditions and initial conditions (1b) for some initial state $\mathbf{m}^0 : \Omega \to \mathbb{R}^3$ with $|\mathbf{m}^0| = 1$. The dynamics of the spin accumulation $\mathbf{s}$ is governed by the diffusion equation [3, 8]

$$\partial_t \mathbf{s} = -\nabla \cdot \mathbf{J}_{\text{s}} - \frac{2D_0}{\lambda_{\text{sf}}^2}\mathbf{s} - \frac{2D_0}{\lambda_{\text{J}}^2}\mathbf{s} \times \mathbf{m} \quad \text{in } \Omega'_T, \tag{2a}$$

$$\partial_{\mathbf{n}} \mathbf{s} = \mathbf{0} \text{ on } (0,T) \times \partial\Omega', \quad \mathbf{s}(0) = \mathbf{s}^0 \text{ in } \Omega'. \tag{2b}$$

Here, D_0 denotes the diffusion coefficient, $\lambda_{\text{sf}}, \lambda_{\text{J}} > 0$ are characteristic lengths, and $\mathbf{s}^0 : \Omega' \to \mathbb{R}^3$ is some initial configuration. The spin current $\mathbf{J}_{\text{s}}$ reads

$$\mathbf{J}_{\text{s}} = \frac{\beta \mu_{\text{B}}}{e} \mathbf{m} \otimes \mathbf{J}_{\text{e}} - 2D_0 \left(\nabla \mathbf{s} - \beta\beta' \mathbf{m} \otimes (\nabla \mathbf{s}^\top \mathbf{m}) \right) \quad \text{in } \Omega'_T, \tag{2c}$$

where $\mathbf{J}_{\text{e}} : \Omega'_T \to \mathbb{R}^3$ is a given electric current density and the constants $\mu_{\text{B}} > 0$, $e > 0$, and $0 < \beta, \beta' < 1$ are the Bohr magneton, the electron electric charge, and polarization parameters, respectively. The above setting covers the case of multilayer structures, where Ω' denotes the volume of the entire multilayer sample, while Ω denotes its ferromagnetic part (see Section 4).

Existence of weak solutions of the nonlinear system (1)–(2) has been established in [8]. A first numerical scheme based on finite differences has been proposed and empirically validated in [9]. A convergent finite element integrator has been proposed, analyzed, and applied by the authors in [10, 11]. The latter scheme extends the integrator of [12] and is unconditionally convergent towards a weak solution of the system, although each time-step decouples the integration of (1) and (2) and requires only to solve two linear systems (despite the overall nonlinearities).

The dynamics of the spin accumulation is much faster than the one of the magnetization [3]. If one is only interested in the magnetization dynamics, it is thus reasonable to treat the spin accumulation as in equilibrium, i.e., to consider the stationary

*Corresponding author.
Email address: michele.ruggeri@tuwien.ac.at (Michele Ruggeri)

case of the governing diffusion equation. With this approach, the time-dependent equation (2) reduces to the boundary value problem

$$
\begin{aligned}
&-\nabla\cdot\Big(D_0(\nabla\mathbf{s}-\beta\beta'\mathbf{m}\otimes(\nabla\mathbf{s}^\top\mathbf{m}))\Big)+\frac{D_0}{\lambda_{\mathrm{sf}}^2}\mathbf{s}+\frac{D_0}{\lambda_{\mathrm{J}}^2}(\mathbf{s}\times\mathbf{m})\\
&\quad=-\frac{\beta\mu_{\mathrm{B}}}{2e}\nabla\cdot(\mathbf{m}\otimes\mathbf{J}_{\mathrm{e}})\quad\text{in }\Omega',
\end{aligned}
\tag{3a}
$$

$$
\partial_{\mathbf{n}}\mathbf{s}=0\quad\text{on }\partial\Omega'. \tag{3b}
$$

In the present work, as a novel contribution over [8–11], we analyze the numerical integration of (1) coupled to (3). We prove convergence of the algorithm towards a weak solution of the problem and compare the numerical results with those for (1)–(2). The latter is computationally more expensive, since it requires a smaller time-step size in order to resolve the dynamics of the spin accumulation.

2. Variational formulation and weak solution

We assume that $D_0\in L^\infty(\Omega')$ satisfies $D_0\geq D_*$ a.e. in Ω' for a positive constant D_*. For the moment, we omit the time-dependence of all quantities, assume $\mathbf{J}_{\mathrm{e}}\in\mathbf{H}(\mathrm{div},\Omega')$, and consider the set $\mathcal{M}=\{\mathbf{m}\in\mathbf{L}^\infty(\Omega):|\mathbf{m}|\leq 1\text{ a.e. in }\Omega\}$. For $\mathbf{m}\in\mathcal{M}$, we define the bilinear form $a_{\mathbf{m}}:\mathbf{H}^1(\Omega')\times\mathbf{H}^1(\Omega')\to\mathbb{R}$ by

$$
\begin{aligned}
a_{\mathbf{m}}(\boldsymbol{\zeta}_1,\boldsymbol{\zeta}_2)&=(D_0\nabla\boldsymbol{\zeta}_1,\nabla\boldsymbol{\zeta}_2)_{\Omega'}-\beta\beta'(D_0\mathbf{m}\otimes(\nabla\boldsymbol{\zeta}_1^\top\mathbf{m}),\nabla\boldsymbol{\zeta}_2)_\Omega\\
&\quad+\lambda_{\mathrm{sf}}^{-2}(D_0\boldsymbol{\zeta}_1,\boldsymbol{\zeta}_2)_{\Omega'}+\lambda_{\mathrm{J}}^{-2}(D_0(\boldsymbol{\zeta}_1\times\mathbf{m}),\boldsymbol{\zeta}_2)_\Omega.
\end{aligned}
\tag{4}
$$

for all $\boldsymbol{\zeta}_1,\boldsymbol{\zeta}_2\in\mathbf{H}^1(\Omega')$. The variational formulation of (3) then reads as follows: Find $\mathbf{s}\in\mathbf{H}^1(\Omega')$ such that, for all $\boldsymbol{\zeta}\in\mathbf{H}^1(\Omega')$, it holds

$$
a_{\mathbf{m}}(\mathbf{s},\boldsymbol{\zeta})=\frac{\beta\mu_{\mathrm{B}}}{2e}(\mathbf{m}\otimes\mathbf{J}_{\mathrm{e}},\nabla\boldsymbol{\zeta})_\Omega-\frac{\beta\mu_{\mathrm{B}}}{2e}(\mathbf{J}_{\mathrm{e}}\cdot\mathbf{n},\mathbf{m}\cdot\boldsymbol{\zeta})_{\partial\Omega'\cap\partial\Omega}. \tag{5}
$$

The following proposition characterizes the mapping $\mathbf{m}\mapsto\mathbf{s}$.

Proposition 1. *For all $\mathbf{m}\in\mathcal{M}$, there exists a unique solution $\mathbf{s}\in\mathbf{H}^1(\Omega')$ of (5). Moreover, it holds*

$$
\|\mathbf{s}\|_{\mathbf{H}^1(\Omega')}\leq\frac{\beta\mu_{\mathrm{B}}\|\mathbf{J}_{\mathrm{e}}\|_{\mathbf{H}(\mathrm{div},\Omega')}}{2D_*|e|\min\{1-\beta\beta',\lambda_{\mathrm{sf}}^{-2}\}}.
$$

Proof. Recall $|\mathbf{m}|\leq 1$ a.e. in Ω. It follows that the bilinear form $a_{\mathbf{m}}(\cdot,\cdot)$ is continuous and coercive, as $a_{\mathbf{m}}(\boldsymbol{\zeta},\boldsymbol{\zeta})\geq D_*\min\{1-\beta\beta',\lambda_{\mathrm{sf}}^{-2}\}\|\boldsymbol{\zeta}\|^2_{\mathbf{H}^1(\Omega)}$ for all $\boldsymbol{\zeta}\in\mathbf{H}^1(\Omega')$. Moreover, $F(\cdot)$ defined as the right-hand side of (5) is linear and continuous, as $|F(\boldsymbol{\zeta})|\leq(\beta\mu_{\mathrm{B}}|e|^{-1}/2)\,\|\mathbf{J}_{\mathrm{e}}\|_{\mathbf{H}(\mathrm{div},\Omega')}\|\boldsymbol{\zeta}\|_{\mathbf{H}^1(\Omega)}$ for all $\boldsymbol{\zeta}\in\mathbf{H}^1(\Omega')$. Therefore, the result follows from the Lax-Milgram theorem. □

We suppose $\mathbf{f}\in C([0,T];\mathbf{L}^2(\Omega))$ and $\mathbf{J}_{\mathrm{e}}\in C([0,T],\mathbf{H}(\mathrm{div},\Omega'))$. In the spirit of [13–15], we introduce the notion of a weak solution of (1) coupled to (3):

Definition 2. *Let $\mathbf{m}^0\in\mathbf{H}^1(\Omega)$ with $|\mathbf{m}^0|=1$ a.e. in Ω. Then, $\mathbf{m}:\Omega_T\to\mathbb{R}^3$ is called a weak solution of the coupling of* (1) *and* (3) *if the following properties* (i)–(iv) *are satisfied:*

(i) $\mathbf{m}\in\mathbf{H}^1(\Omega_T)$ *and* $|\mathbf{m}|=1$ *a.e. in* Ω_T,

(ii) $\mathbf{m}(0)=\mathbf{m}^0$ *in the sense of traces,*

(iii) *for all* $\boldsymbol{\varphi}\in\mathbf{H}^1(\Omega_T)$, *it holds*

$$
\begin{aligned}
&(\partial_t\mathbf{m},\boldsymbol{\varphi})_{\Omega_T}+\alpha\,(\partial_t\mathbf{m}\times\mathbf{m},\boldsymbol{\varphi})_{\Omega_T}\\
&\quad=-C_{\mathrm{exch}}\gamma_0\,(\nabla\mathbf{m}\times\mathbf{m},\nabla\boldsymbol{\varphi})_{\Omega_T}+\gamma_0\,(\boldsymbol{\pi}(\mathbf{m})\times\mathbf{m},\boldsymbol{\varphi})_{\Omega_T}\\
&\qquad+\gamma_0\,(\mathbf{f}\times\mathbf{m},\boldsymbol{\varphi})_{\Omega_T}+c\gamma_0\,(\mathbf{s}\times\mathbf{m},\boldsymbol{\varphi})_{\Omega_T},
\end{aligned}
$$

(iv) *for a.e. time* $T'\in(0,T)$, *it holds*

$$
\|\nabla\mathbf{m}(T')\|^2_{\mathbf{L}^2(\Omega)}+\alpha\int_0^{T'}\|\partial_t\mathbf{m}(t)\|^2_{\mathbf{L}^2(\Omega)}\mathrm{d}t\leq C, \tag{6}
$$

where the constant $C>0$ depends only on the data.

We point out that stronger (dissipative) bounds than (6) in terms of the Gibbs free energy require additional assumptions on $\boldsymbol{\pi}$ and $\mathbf{f}$; see [14, 15].

3. Numerical algorithm

For the spatial discretization, let $\{\mathcal{T}_h^{\Omega'}\}_{h>0}$ be a quasi-uniform family of conforming tetrahedral triangulations of Ω' with meshsize h. We assume that Ω is resolved, i.e., the restriction $\mathcal{T}_h^\Omega=\big\{K\in\mathcal{T}_h^{\Omega'}:K\subseteq\overline{\Omega}\big\}$ satisfies $\overline{\Omega}=\bigcup_{K\in\mathcal{T}_h^\Omega}K$. We denote by $\mathbf{V}_h(\Omega')=\mathcal{S}^1(\mathcal{T}_h^{\Omega'})^3$ the standard finite element space of globally continuous and piecewise affine functions from Ω' to $\mathbb{R}^3$ and define $\mathbf{V}_h(\Omega)$ analogously. The set of vertices of the triangulation $\mathcal{T}_h^\Omega$ is denoted by $\mathcal{N}_h^\Omega$. We define the set of admissible discrete magnetizations by

$$
\mathcal{M}_h:=\big\{\boldsymbol{\phi}_h\in\mathbf{V}_h(\Omega):|\boldsymbol{\phi}_h(\mathbf{z})|=1\text{ for all }\mathbf{z}\in\mathcal{N}_h^\Omega\big\}\subset\mathcal{M}
$$

and consider, for $\boldsymbol{\phi}_h\in\mathcal{M}_h$, the discrete tangent space

$$
\mathcal{K}_{\boldsymbol{\phi}_h}:=\big\{\boldsymbol{\psi}_h\in\mathbf{V}_h(\Omega):\boldsymbol{\psi}_h(\mathbf{z})\cdot\boldsymbol{\phi}_h(\mathbf{z})=0\text{ for all }\mathbf{z}\in\mathcal{N}_h^\Omega\big\}.
$$

We note that these definitions are inspired by mimicking the properties $|\mathbf{m}|=1$ and $\mathbf{m}\cdot\partial_t\mathbf{m}=\frac{1}{2}\,\partial_t|\mathbf{m}|^2=0$ a.e. in Ω_T which are satisfied for each solution $\mathbf{m}$ of (1).

For the time discretization, we consider a uniform partition of the time interval $[0,T]$ with time-step size $\Delta t=T/N$, i.e., $t_i=i\Delta t$ for $0\leq i\leq N$. Algorithm 3 approximates $\mathbf{m}(t_i)\approx\mathbf{m}_h^i\in\mathcal{M}_h$ as well as $\partial_t\mathbf{m}(t_i)\approx\mathbf{v}_h^i\in\mathcal{K}_{\mathbf{m}_h^i}$. Instead of (5), we consider the following discrete problem: Given $\mathbf{J}_{\mathrm{e}}^i:=\mathbf{J}_{\mathrm{e}}(t_i)$, find $\mathbf{s}_h^i\in\mathbf{V}_h(\Omega')$ such that, for all $\boldsymbol{\zeta}_h\in\mathbf{V}_h(\Omega')$, it holds

$$
a_{\mathbf{m}_h^i}(\mathbf{s}_h^i,\boldsymbol{\zeta}_h)=\frac{\beta\mu_{\mathrm{B}}}{2e}(\mathbf{m}_h^i\otimes\mathbf{J}_{\mathrm{e}}^i,\nabla\boldsymbol{\zeta}_h)_\Omega-\frac{\beta\mu_{\mathrm{B}}}{2e}(\mathbf{J}_{\mathrm{e}}^i\cdot\mathbf{n},\mathbf{m}_h^i\cdot\boldsymbol{\zeta}_h)_{\partial\Omega'\cap\partial\Omega}. \tag{7}
$$

Arguing as for Proposition 1, we see that (7) is well-posed and that $\mathbf{s}_h^i\in\mathbf{V}_h(\Omega')$ satisfies

$$
\|\mathbf{s}_h^i\|_{\mathbf{H}^1(\Omega')}\leq\frac{\beta\mu_{\mathrm{B}}\|\mathbf{J}_{\mathrm{e}}\|_{C([0,T],\mathbf{H}(\mathrm{div},\Omega'))}}{2D_*|e|\min\{1-\beta\beta',\lambda_{\mathrm{sf}}^{-2}\}}. \tag{8}
$$

Let $\mathbf{m}_h^0\in\mathcal{M}_h$ be a suitable discretization of the initial condition which satisfies $\mathbf{m}_h^0\rightharpoonup\mathbf{m}^0$ in $\mathbf{H}^1(\Omega)$ as $h\to 0$. Assume that the general contribution $\boldsymbol{\pi}(\mathbf{m})$ is approximated by

$\boldsymbol{\pi}_h : \mathcal{M}_h \to \mathbf{L}^2(\Omega)$ such that $\|\boldsymbol{\pi}_h(\boldsymbol{\phi}_h)\|_{\mathbf{L}^2(\Omega)} \le C$ for all $\boldsymbol{\phi}_h \in \mathcal{M}_h$, and $\boldsymbol{\pi}_h(\boldsymbol{\phi}_h) \rightharpoonup \boldsymbol{\pi}(\boldsymbol{\phi})$ in $\mathbf{L}^2(\Omega)$ whenever $\boldsymbol{\phi}_h \to \boldsymbol{\phi}$ in $\mathbf{L}^2(\Omega)$. This general framework for the discretization of general $\mathbf{m}$-dependent field contributions has been introduced in [15] and covers many classical strategies, e.g., the hybrid FEM/BEM method from [16] for the computation of the stray field. For the numerical integration of the coupling of (1) and (3), we propose the following algorithm, where $\mathbf{f}^i := \mathbf{f}(t_i)$.

Algorithm 3. *For all $0 \le i \le N-1$ iterate the steps* (i)–(iii)*:*

(i) *Compute $\boldsymbol{\pi}_h(\mathbf{m}_h^i) \in \mathbf{V}_h(\Omega)$, compute $\mathbf{s}_h^i \in \mathbf{V}_h(\Omega')$ from* (7)*.*

(ii) *Compute $\mathbf{v}_h^i \in \mathcal{K}_{\mathbf{m}_h^i}$ such that, for all $\boldsymbol{\phi}_h \in \mathcal{K}_{\mathbf{m}_h^i}$, it holds*

$$\begin{aligned} &\alpha\left(\mathbf{v}_h^i, \boldsymbol{\phi}_h\right)_\Omega + \left(\mathbf{m}_h^i \times \mathbf{v}_h^i, \boldsymbol{\phi}_h\right)_\Omega + C_{\mathrm{exch}}\gamma_0\theta\Delta t\left(\nabla \mathbf{v}_h^i, \nabla\boldsymbol{\phi}_h\right)_\Omega \\ &\quad = -C_{\mathrm{exch}}\gamma_0\left(\nabla \mathbf{m}_h^i, \nabla\boldsymbol{\phi}_h\right)_\Omega + \gamma_0\left(\boldsymbol{\pi}_h(\mathbf{m}_h^i), \boldsymbol{\phi}_h\right)_\Omega \\ &\qquad + \gamma_0\left(\mathbf{f}^i, \boldsymbol{\phi}_h\right)_\Omega + c\gamma_0\left(\mathbf{s}_h^i, \boldsymbol{\phi}_h\right)_\Omega. \end{aligned} \tag{9}$$

(iii) *Define $\mathbf{m}_h^{i+1} \in \mathcal{M}_h$ by*

$$\mathbf{m}_h^{i+1}(\mathbf{z}) = \frac{\mathbf{m}_h^i(\mathbf{z}) + \Delta t\, \mathbf{v}_h^i(\mathbf{z})}{|\mathbf{m}_h^i(\mathbf{z}) + \Delta t\, \mathbf{v}_h^i(\mathbf{z})|} \quad \text{for all } \mathbf{z} \in \mathcal{N}_h^\Omega.$$

The algorithm combines the tangent plane scheme [12, 14, 15] with (7). We note that (9) fits in the form of the Lax-Milgram theorem and thus admits a unique solution $\mathbf{v}_h^i \in \mathcal{K}_{\mathbf{m}_h^i}$. In particular, it holds $|\mathbf{m}_h^i + \Delta t\, \mathbf{v}_h^i|^2 = 1 + \Delta t^2 |\mathbf{v}_h^i|^2 \ge 1$. It follows that Algorithm 3 is well-defined for all discretization parameters $h, \Delta t > 0$. Overall, only two well-posed linear systems are solved per time-step, although the system is nonlinear in $\mathbf{m}$ and nonlinearly coupled with $\mathbf{s}$.

The output $\{\mathbf{m}_h^i\}_{0\le i\le N}$ of Algorithm 3 induces the piecewise linear time approximation of the magnetization defined by

$$\mathbf{m}_{h\Delta t}(t) := \frac{t - t_i}{\Delta t}\mathbf{m}_h^{i+1} + \frac{t_{i+1} - t}{\Delta t}\mathbf{m}_h^i$$

for all $t \in [t_i, t_{i+1}]$, $0 \le i \le N-1$. To see that the sequence $\{\mathbf{m}_{h\Delta t}\}_{h,\Delta t>0}$ converges towards a weak solution in the sense of Definition 2, we apply the framework for general effective field contributions introduced in [15].

Theorem 4. *Suppose that any mesh of the family $\{\mathcal{T}_h^{\Omega'}\}_{h>0}$ satisfies the angle condition*

$$(\nabla\varphi_{\mathbf{z}}, \nabla\varphi_{\mathbf{z}'})_\Omega \le 0 \quad \text{for all distinct vertices } \mathbf{z}, \mathbf{z}' \in \mathcal{N}_h^\Omega. \tag{10}$$

Then, the sequence $\{\mathbf{m}_{h\Delta t}\}_{h,\Delta t>0}$ converges, upon extraction of a subsequence, weakly in $\mathbf{H}^1(\Omega_T)$ towards a weak solution of the LLG equation in the sense of Definition 2 as $h, \Delta t \to 0$. If $1/2 < \theta \le 1$, the convergence is unconditional.

Proof. The proof uses the same arguments as in [12, 14, 15]. Therefore, we only sketch it. In particular, the result follows from [15, Theorem 3.1], once we show that $\|\mathbf{s}_h^i\|_{\mathbf{L}^2(\Omega')} \le C$ for all $0 \le i \le N-1$, see [15, equation (3.12)], and that the piecewise constant time approximation of the spin accumulation defined by $\mathbf{s}_{h\Delta t}^-(t) := \mathbf{s}_h^i$ for all $t \in [t_i, t_{i+1})$, $0 \le i \le N-1$ satisfies the convergence property $\mathbf{s}_{h\Delta t}^- \rightharpoonup \mathbf{s}$ in $\mathbf{L}^2(\Omega_T')$ as $h, \Delta t \to 0$, see [15, equation (3.13)]. The first condition directly follows from (8). From (8), we also obtain that the sequence $\{\mathbf{s}_{h\Delta t}^-\}_{h,\Delta t>0}$ is uniformly bounded in $\mathbf{L}^\infty(0, T; \mathbf{H}^1(\Omega'))$. In particular, we deduce that, upon extraction of a subsequence, $\mathbf{s}_{h\Delta t}^- \rightharpoonup \tilde{\mathbf{s}}$ in $\mathbf{L}^2(\Omega_T')$ for some $\tilde{\mathbf{s}} \in \mathbf{L}^2(\Omega_T')$. Exploiting the fact that $\mathbf{m}_{h\Delta t} \to \mathbf{m}$ in $\mathbf{L}^2(\Omega_T)$, the identification of $\tilde{\mathbf{s}}$ with the solution $\mathbf{s}$ of (5) is obtained by passing to the limit (7) for $h, \Delta t \to 0$. □

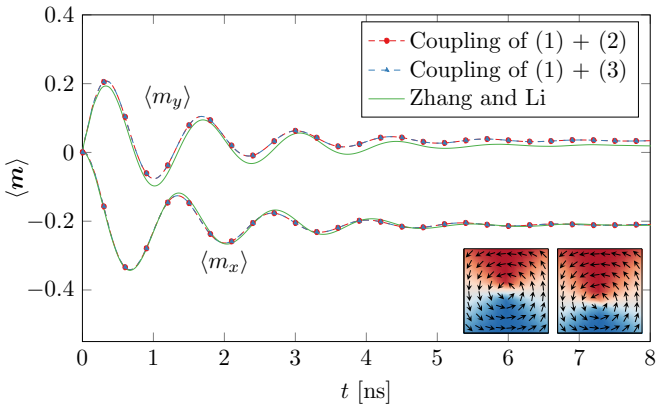

Figure 1: μMAG standard problem #5. Damped gyration of a magnetic vortex under the influence of a DC current. The results of Algorithm 3 are compared to the nonequilibrium algorithm which discretizes the coupling of (1) and (2) proposed in [10, 11] and the model of Zhang and Li [5]. The insets depict the equilibrium configuration of the vortex without and with applied current.

Remark 5. *The angle condition* (10) *is a technical assumption that is required for the convergence analysis of Algorithm 3. It is needed to ensure the H^1-stability of the nodewise projection from step* (iii) *[17]. In 3D, a sufficient condition for* (10) *is that all angles between faces of tetrahedra are bounded by $\pi/2$. If the triangulation does not satisfies the angle condition, then the convergence proof requires the discretization parameters to satisfy the CFL condition $\Delta t\, h^{-2} \le C$. However, extended numerical experiments show that the method seems to be stable even if the angle condition is violated. This might signify that assumption* (10) *is only an artifact of the proof technique.*

Remark 6. *Arguing along the lines of [10], one can show that the projection step can be omitted. The constraint then fails to hold at the nodes of the triangulation, but the violation is uniformly bounded by the time-step size, independently of the number of iterations. In particular, the limit of $\mathbf{m}$ of $\{\mathbf{m}_{h\Delta t}\}_{h,\Delta t>0}$ satisfies $|\mathbf{m}| = 1$ a.e. in Ω_T also in this case. However, the projection step must be included in the definition* (4) *of the bilinear form $a_{\mathbf{m}_h^i}(\cdot,\cdot)$ in order to preserve its coercivity. Then, Theorem 4 remains valid even if the triangulation does not satisfies the angle condition* (10)*.*

4. Numerical experiments

In this section, we compare the simulation results of Algorithm 3, which integrates the coupling of (1) and (3) with the algorithm proposed in [10, 11] which discretizes (1)–(2).

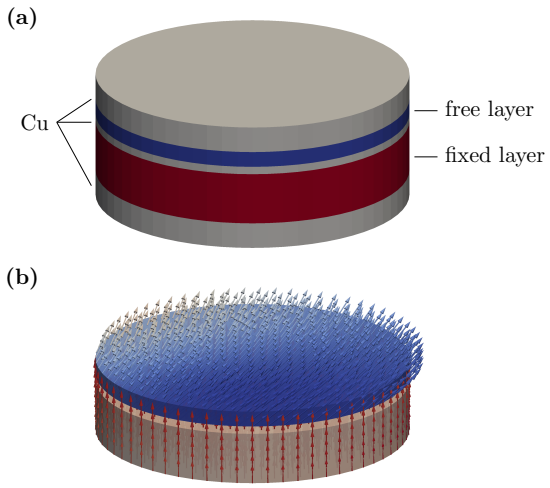

Figure 2: Spin-torque oscillator. (a) Material stack. (b) Magnetization configuration during oscillation.

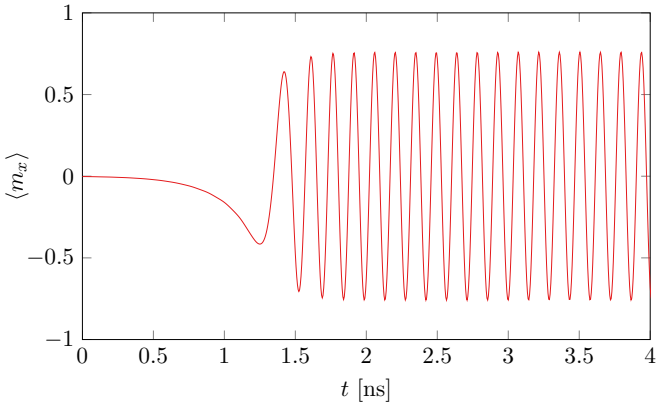

Figure 3: Averaged x-component of the magnetization in the free layer of the spin-torque oscillator. A stable oscillation with $f \approx 6.86\,\mathrm{GHz}$ is established after a short transient period.

A suitable benchmark for current driven domain-wall motion is the micromagnetic standard problem #5 proposed by the μMAG group [18]. A thin square of size $100 \times 100 \times 10\,\mathrm{nm}^3$ with material parameters of permalloy ($M_s = 8 \times 10^5\,\mathrm{A/m}$, $A = 1.3 \times 10^{-11}\,\mathrm{J/m}$, $\alpha = 0.1$) is prepared in a magnetic vortex state. A homogeneous DC current in x-direction is then applied, which leads to a damped gyration of the vortex core around a shifted equilibrium. While the μMAG group proposes to solve this problem with the model of Zhang and Li [5], we use the presented diffusion model with an equivalent choice of current-related material parameters [11], i.e., $D_0 = 1 \times 10^{-3}\,\mathrm{m/s^2}$, $\beta = 0.9$, $\beta' = 0.8$, $\lambda_{\mathrm{sf}} = 10\,\mathrm{nm}$, $\lambda_{\mathrm{J}} = 2.236\,\mathrm{nm}$, $c = 3.155 \times 10^{-3}\,\mathrm{N/A^2}$. The simulations are carried out with the time-step $\Delta t = 1 \times 10^{-13}\,\mathrm{s}$, the results are shown in Figure 1. While the results of the considered model slightly differ from the Zhang and Li solution, there is no notable difference between the coupling with the time-dependent spin diffusion (2) and with the equilibrium ansatz (3). This justifies the simplified equilibrium treatment of the spin accumulation.

As a second benchmark, we consider the circular multilayer structure depicted in Figure 2(a) with diameter 60 nm and layer thicknesses $\{5, 3, 1.5, 10, 5\}\,\mathrm{nm}$ from top to bottom. The 3 nm free layer has soft magnetic properties, i.e., $M_s = 7.96 \times 10^5\,\mathrm{A/m}$, $A = 2.8 \times 10^{-11}\,\mathrm{J/m}$, $K = 0$, $\alpha = 0.012$. The 10 nm fixed layer has similar properties, but higher saturation magnetization $M_s = 9.87 \times 10^5\,\mathrm{A/m}$ as well as uniaxial anisotropy with $K = 1 \times 10^6\,\mathrm{J/m^3}$ and easy axis in the z-direction (perpendicular to the stack interfaces). The diffusion parameters in the magnetic material are chosen similarly to those of the standard problem #5. The same parameters are used for the nonmagnetic regions, except for a higher diffusion constant $D_0 = 5 \times 10^{-3}\,\mathrm{m/s^2}$. The system is simulated under the influence of an external field in z-direction with $\mu_0|\mathbf{H}_{\mathrm{ext}}| = 0.6\,\mathrm{T}$ and a DC current in z-direction with a density of $|\mathbf{J}_{\mathrm{e}}| = 4 \times 10^{11}\,\mathrm{A/m^2}$. The simulation is carried out with the time-step $\Delta t = 1 \times 10^{-13}\,\mathrm{s}$, the corresponding results are shown in Figure 3. After a short transient period, the magnetization in the free layer performs a stable oscillation with a frequency $f \approx 6.86\,\mathrm{GHz}$. A typical magnetization state during the oscillation is depicted in Figure 2(b). This oscillation originates in the spin torque excerted on the free layer by itinerant electrons that are polarized in the fixed layer.

5. Conclusions

We have introduced a mathematically convergent integrator for the coupling of the LLG equation and a stationary drift-diffusion equation for the spin accumulation. The numerical experiments demonstrate how the presented model can be used to describe the spin torque in both multilayer structures and domain walls. Furthermore, it is shown that in order to describe the magnetization dynamics accurately it is sufficient to treat the spin accumulation in equilibrium in contrast to the full dynamic description considered in [8–11]. Within the considered approach, the electric current density is assumed to be given. Future work in the direction of a fully self-consistent model will include also the computation of the current, in order to take also the influence of the magnetization configuration to the electrical resistance into account. This will be achieved by coupling (1) and (3) with a suitable form of the Maxwell equations.

Acknowledgments

The authors acknowledge support of the Vienna Science and Technology Fund (WWTF) under grant MA14-44 (GH, DP, DS), of the Austrian Science Fund (FWF) under grant W1245 (DP, MR), of TU Wien through the innovative projects initiative (DP, MR), of the Austrian Federal Ministry of Science, Research and Economy and the National Foundation for Research, Technology and Development (CA, DS), through the EPSRC grant EP/K008412/1 (GH), of the Royal Society under grant UF080837 (GH).

References

[1] J. C. Slonczewski, Current-driven excitation of magnetic multilayers, J. Magn. Magn. Mat. 159 (1996) L1–L7.

[2] L. Berger, Emission of spin waves by a magnetic multilayer traversed by a current, Phys. Rev. B 54 (1996) 9353–9358.

[3] S. Zhang, P. M. Levy, A. Fert, Mechanisms of spin-polarized current-driven magnetization switching, Phys. Rev. Lett. 88 (2002) 236601.

[4] A. Shpiro, P. M. Levy, S. Zhang, Self-consistent treatment of nonequilibrium spin torques in magnetic multilayers, Phys. Rev. B 67 (2003) 104430.

[5] S. Zhang, Z. Li, Roles of nonequilibrium conduction electrons on the magnetization dynamics of ferromagnets, Phys. Rev. Lett. 93 (2004) 127204.

[6] K.-J. Lee, M. D. Stiles, H.-W. Lee, J.-H. Moon, K. K.-W., S.-W. Lee, Self-consistent calculation of spin transport and magnetization dynamics, Phys. Rep. 531 (2013) 89–113.

[7] P. Chureemart, I. D'Amico, R. W. Chantrell, Model of spin accumulation and spin torque in spatially varying magnetisation structures: limitations of the micromagnetic approach, J. Phys.: Condens. Matter 27 (2015) 146004.

[8] C. J. García-Cervera, X.-P. Wang, Spin-polarized transport: Existence of weak solutions, Discrete Contin. Dyn. Syst. Ser. B 7 (2007) 87–100.

[9] C. J. García-Cervera, X.-P. Wang, Spin-polarized currents in ferromagnetic multilayers, J. Comput. Phys. 224 (2007) 699–711.

[10] C. Abert, G. Hrkac, M. Page, D. Praetorius, M. Ruggeri, D. Suess, Spin-polarized transport in ferromagnetic multilayers: An unconditionally convergent FEM integrator, Comput. Math. Appl. 68 (2014) 639–654.

[11] C. Abert, M. Ruggeri, F. Bruckner, C. Vogler, G. Hrkac, D. Praetorius, D. Suess, A three-dimensional spin-diffusion model for micromagnetics, 2014. Submitted for publication, preprint available at arXiv:1410.6067.

[12] F. Alouges, A new finite element scheme for Landau-Lifchitz equations, Discrete Contin. Dyn. Syst. Ser. S 1 (2008) 187–196.

[13] F. Alouges, A. Soyeur, On global weak solutions for Landau-Lifshitz equations: Existence and nonuniqueness, Nonlinear Anal. 18 (1992) 1071–1084.

[14] F. Alouges, E. Kritsikis, J.-C. Toussaint, A convergent finite element approximation for Landau-Lifschitz-Gilbert equation, Physica B 407 (2012) 1345–1349.

[15] F. Bruckner, M. Feischl, T. Führer, P. Goldenits, M. Page, D. Praetorius, M. Ruggeri, D. Suess, Multiscale modeling in micromagnetics: Existence of solutions and numerical integration, Math. Models Methods Appl. Sci. 24 (2014) 2627–2662.

[16] D. R. Fredkin, T. R. Koehler, Hybrid method for computing demagnetization fields, IEEE Trans. Magn. 26 (1990) 415–417.

[17] S. Bartels, Stability and convergence of finite-element approximation schemes for harmonic maps, SIAM J. Numer. Anal. 43 (2005) 220–238.

[18] D. Porter, μMAG standard problem #5, 2014. URL: `http://www.ctcms.nist.gov/~rdm/std5/spec5.xhtml`.